Quasi-Majoranas in inhomogeneous full-shell hybrid nanowires

César Robles[1] and Elsa Prada[1]
[1] *Instituto de Ciencia de Materiales de Madrid (ICMM), CSIC, Madrid, Spain*
(Dated: December 26, 2024)

Unambiguous detection of Majorana zero modes (MZMs) in hybrid nanostructures is still a pending task for the condensed matter physics field. The importance of these states lies in their topological properties, such as strong resilience against local perturbations, which translates into a potential application of MZMs for quantum computation. When smooth disorder is added to the study of hybrid nanostructures, non-topological (or trivial) states can appear at zero energy rather than MZMs. These states, referred to as quasi-Majoranas, can mimic measurable local signatures of MZMs. A recent alternative hybrid nanowire design, candidate for hosting MZMs, is the full-shell nanowire. It consists of a semiconductor nanowire fully coated by a superconductor shell in the presence of a magnetic flux. In this work, we study how the local density of states is affected by an inhomogeneous potential profile at the end of the hybrid wire, in the form of a smooth chemical potential step. We find quasi-Majorana physics, but only in half of the wire's parameter space. In the other half, the system still hosts MZMs, in contrast to what happens in partial-shell conventional Majorana nanowires. The reason can be traced back to the flux-dependent effective chemical potential and effective Zeeman field of the full-shell design.

I. INTRODUCTION

With the introduction of topological band theory, new topological boundary states and their remarkable properties have been the subject of intense research during the last decade. One of these states, that appears at the ends of a one-dimensional topological superconductor (SC), is called a Majorana zero mode (MZM) [1]. MZMs are zero-energy, zero-spin and zero-charge fractional mid-gap quasiparticles that obey non-Abelian statistics. They satisfy the Majorana condition, that is, that its defining operator, $\gamma^\dagger$, is self-conjugate: $\gamma^\dagger = \gamma$. This makes MZMs a very exotic state in condensed matter physics with potential applications in topologically protected quantum computing [2].

One of the most studied platforms capable of hosting MZMs is based on hybrid nanowires. They were introduced by Oreg *et al.* [3] and Lutchyn *et al.* [4] back in 2010 in terms of a simple model known as the Majorana nanowire. Majorana nanowires consist of a semiconducting (SM) core with strong spin-orbit coupling (SOC), partially coated with a conventional SC and subjected to an external axial magnetic field. These interactions give rise to a (p-wave) gap symmetry capable of undergoing a topological transition (TT) driven by the Zeeman effect. As we increase the Zeeman field, the TT manifests itself in the wire's spectrum as a bulk gap closing and reopening at a Zeeman critical value. Once in the topological phase, two midgap zero-energy modes appear in long enough nanowires bound to the wire's ends. All of this phenomenology appears in an ideal, homogeneous Majorana nanowire. However, when studying more realistic wires, it was found that the presence of smooth parameter inhomogeneities along the wire's length gave rise to so-called quasi-Majorana states bound to the inhomogeneities [5]. These states are trivial, in the topological sense, but can mimic the phenomenology of true MZMs in local experimental signatures. In particular, as we will see throughout this work, they appear as zero-energy states in the wire's spectrum.

Recently, a new type of SC-SM nanowire, called a full-shell hybrid nanowire [see Fig. 1(a)], came to the spotlight because of its advantages over previous designs [6]. In this new geometry, a thin SC shell covers all around the SM core forming a superconducting tube, as opposed to what happens in conventional Majorana nanowires, where the SC only partially covers the core. A new effect appears when applying a magnetic field through a tubular (doubly-connected) SC: the Little-Parks (LP) effect. In this effect, the SC critical temperature or, equivalently, the SC gap, varies quasiperiodically with flux Φ, forming a series of so-called LP lobes [7]. Within each lobe, the *fluxoid* is quantized in units of the superconducting flux quantum, $\Phi_0 = h/2e$ [8]. The fluxoid number $n = 0, \pm1, \pm2...$ represents the SC phase winding, i.e. the number of twists that the order parameter's phase acquires as the flux through the tube increases. One consequence of the LP effect is that the driving mechanism for the TT is no longer the Zeeman field, but the flux threading the wire. Another consequence is the LP modulation of the hybrid nanowire energy spectrum. Not only the parent SC, but also all subgap features get modulated with flux through the LP effect.

The phenomenology of homogeneous full-shell hybrid nanowires has been analyzed in recent years, both in the trivial [9] and topological regimes [10], but the effects of disorder in this particular geometry are still unexplored. In this work, we theoretically study for the first time how smooth inhomogeneities of the chemical potential along the wire affect the topological phase and the possibilities of detecting MZMs in full-shell nanowires. In particular, we will study the local density of states (LDOS) when there is chemical potential smooth step close to the wire's end, calculated in different regimes. This quantity is one of the most accessible and measured in experiments in the search for MZMs.

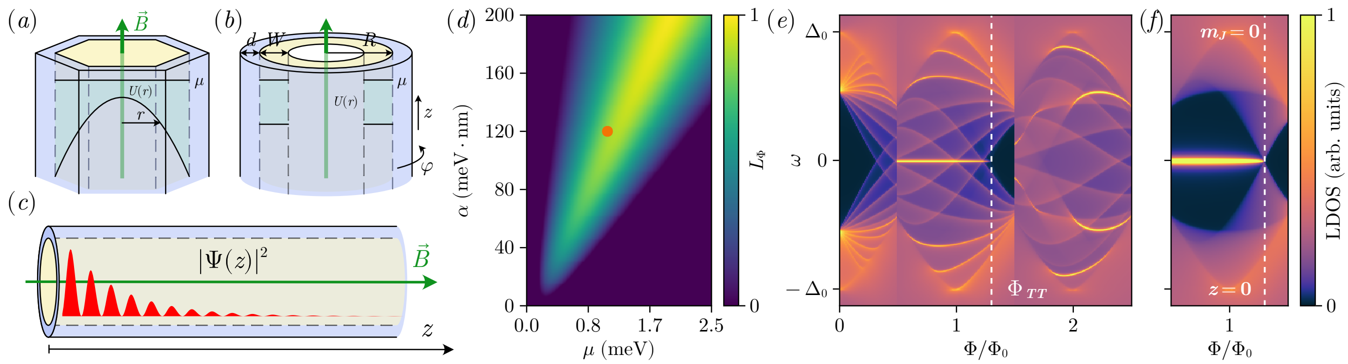

FIG. 1. **Uniform full-shell hybrid nanowire.** (a) Sketch of a realistic full-shell nanowire. A semiconductor (SM) core (yellow) is covered all around by a thin superconductor (SC) shell (blue), both of them with an hexagonal cross section. $U(r)$ is the expected electrostatic potential energy inside the SM, with a maximum at the center of the nanowire. $\vec{B}$ is the applied magnetic field parallel to the wire's axis. (b) Sketch of the nanowire in the cylindrical approximation and in the modified holow-core model (MHCM). The hybrid wire is composed of a SM hollow cylinder of radius R and thickness W encapsulated in a thin SC shell of thickness d. The electrostatic potential $U(r)$ is taken to be constant across the SM. (c) Sketch of the semi-infinite, homogeneous wire along the z direction. In the topological phase, a Majorana bound state appears localized at the end of the wire (not to scale). (d) Topological phase diagram of the first Little-Parks (LP) lobe as a function of chemical potential μ and spin-orbit coupling constant α. The hyperbolic bright shape indicates the topological region, while the dark blue color corresponds to the trivial phase. The color scale L_Φ represents the flux interval of the MZM in the $n = 1$ LP lobe. The dot indicates the parameters chosen for panels (e) and (f). (e) Local density of states (LDOS) at the end ($z = 0$) of a semi-infinite uniform nanowire in the MHCM, in terms of the energy ω and the normalized flux threading the wire Φ/Φ_0. The right half of the $n = 0$ and the full $n = 1$ and $n = 2$ LP lobes are displayed. The vertical dashed line indicates the flux $\Phi_{\rm TT}$ where the topological transition occurs. (f) LDOS of the $n = 1$ lobe showing only the contribution of the $m_J = 0$ subbands. Parameters: $R = 70$ nm, $W = 30$ nm, $\mu = 1.09$ meV, $\alpha = 120$ meV · nm, $\Delta_0 = 0.23$ meV, $\xi_d = 70$ nm, $m^* = 0.023 m_e$, and $a_0 = 5$ nm.

II. THEORETICAL MODEL

A. Effective Hamiltonian and numerical methods

We begin by introducing the theoretical model of a full-shell nanowire. Although fabricated full-shell nanowires usually display a hexagonal cross section, see Fig. 1(a), we can study nanowires with cylindrical symmetry to a very good approximation, so the equations will be written in terms of the (r, φ, z) coordinates. The nanowire is composed of a SM core of radius R and a SC shell of thickness d, as in Fig. 1(b). It is subjected to an axial magnetic field, $\vec{B} = B\hat{z}$, so that the flux threading the wire is $\Phi = \pi R_{\rm LP}^2 B$, where $R_{\rm LP} = R + d/2$. It is taken in a mean radius of the shell, $R_{\rm LP}$. We will be working in the limit of a very thin SC, such that $d \to 0$ and $R_{\rm LP} = R$. Other components of the Hamiltonian are the SM SOC α, the chemical potential μ and, in general, an electrostatic potential $U(r)$ across the wire's cross-section. It can be seen that this type of Hamiltonian commutes with a generalized angular momentum and therefore defines a new quantum number m_J for the energy eigenstates. It takes the values

$$m_J \in \begin{cases} \mathbb{Z} & \text{if } n \text{ is odd.} \\ \mathbb{Z} + 1/2 & \text{if } n \text{ is even,} \end{cases} \tag{1}$$

where $n(\Phi) = \lfloor \Phi/\Phi_0 \rceil = 0, \pm 1, \pm 2$ is the fluxoid number and also labels the LP lobes. MZMs, being zero-energy excitations, can only appear from the $m_J = 0$ subband [6], so we can only find MZMs for odd values of n. Because superconductivity is weakened by a magnetic field, we will be focusing on the first LP lobe, the one with lowest flux which can hold a MZM.

The projection over the m_J eigenstates transforms the initial Hamiltonian into a φ-independent one. The electrostatic potential $U(r)$ is expected to have a dome-like profile, as sketched in Fig. 1(a). The charge thus accumulates near the SM-SC interface in a tubular region of width W [see Fig. 1(b)]. It has been shown that it is possible to consider that all the charge is concentrated at an average radius $R_{\rm av} = R - W/2$. This is the modified hollow-core approximation (MHCA) presented in Ref. [10]. Following App. A and B from Ref. [10] one can arrive to an *effective* Hamiltonian (taking $\hbar = 1$)

$$H = \left(\frac{k_z^2}{2m^*} - \mu_{m_J}\right)\sigma_0\tau_z + V_Z^\phi \sigma_z\tau_0 + A_{m_J}\sigma_0\tau_0 + C_{m_J}\sigma_z\tau_z + \alpha p_z \sigma_y \tau_z + \Sigma_{\rm shell}(\omega), \tag{2}$$

where

$$\mu_{m_J} = \mu - \frac{\alpha}{2R_{\rm av}} - \frac{1}{8m^* R_{\rm av}^2}(4m_J^2 + 1 + \phi^2), \tag{3}$$

$$V_Z^\phi = \frac{1}{2}\phi\left(\frac{1}{2m^* R_{\rm av}^2} + \frac{\alpha}{R_{\rm av}}\right), \tag{4}$$

$$A_{m_J} = -\frac{m_J \phi}{2m^* R_{\rm av}^2}, \tag{5}$$

$$C_{m_J} = -m_J\left(\frac{1}{2m^* R_{\rm av}^2} + \frac{\alpha}{R_{\rm av}}\right). \quad (6)$$

Here, k_z is the momentum operator in the z direction, m^* is the electron effective mass, σ_i and τ_i are the Pauli matrices for the spin and electron-hole spaces, respectively, $\phi = n - \Phi/\Phi_0$ and μ absorbs $U(R_{\rm av})$ into it.

To save resources, the SC is integrated out and implemented as a self-energy $\Sigma_{\rm shell}(\omega)$. In Eq. (2) it takes the form

$$\Sigma_{\rm shell}(\omega) = \Gamma\sigma_0 \frac{\tau_x - u(\omega)\tau_0}{\sqrt{1-u(\omega)^2}}, \quad (7)$$

where Γ is the decay rate of electrons from the core to the shell and $u(\omega)$ is a complex function that, apart from energy ω, depends on flux Φ, the fluxoid number n, the SC gap at zero magnetic field, Δ_0, and the diffusive SC coherence length ξ_d [10].

The Hamiltonian in Eq. (2) includes a derivative in the z coordinate. We can discretize it into a lattice with spacing a_0, and therefore obtain a tight-binding Hamiltonian. The Hamiltonian matrix can now be used to calculate the Green's function of the system, $G = (\omega - H)^{-1}$, to then calculate our required observable, the LDOS as $\mathrm{LDOS}(\omega) = -(1/\pi)\mathrm{Im}[\mathrm{Tr}(G)]$. We have used the Julia packages *Quantica* [11] and *FullShell* [12] to construct the tight-binding model for a full-shell nanowire and to calculate its LDOS, and the package *Makie* [13] to plot the results.

B. Homogeneous wire

For $m_J = 0$ there is a mapping between Eq. (3) and the 1D Majorana nanowire. Using this mapping, we can calculate the condition for the TT in the full-shell nanowire as $V_Z^{\phi} = \sqrt{\mu_{m_J}^2 + \Delta_0^2}$. By writing out this equation in terms of Φ and setting $n = 1$, it has been shown that [10]

$$\frac{\Phi_{\rm TT}}{\Phi_0} = \left(1 - \sqrt{1 + 4m^* R_{\rm av}(\alpha + 2m^* R_{\rm av}\alpha^2 + 2R_{\rm av}\mu) - 4R_{\rm av}\sqrt{m^*\left[(1+2m^* R_{\rm av}\alpha)^2(m^*\alpha^2 + 2\mu) - 4m^* {R_{\rm av}}^2\Delta_0^2\right]}}\right)\left(\frac{R_{\rm LP}}{R_{\rm av}}\right)^2. \quad (8)$$

Using Eq. (8), in Fig. 1(d) we plot the topological phase diagram as a function of μ and α. That is, the (μ, α) points for which $\Phi_{\rm TT}$ is inside the first lobe (bright colored region), for some $R_{\rm av}$. The color bar represents the *length* (in flux units) of the MZM, L_Φ. It is the (normalized) distance from the left-most part of the first lobe ($\Phi/\Phi_0 = 0.5$) to $\Phi_{\rm TT}$. It has no units and is bounded between 0 and 1.

Next, in Fig. 1(e), we plot the LDOS at the end ($z = 0$) of a semi-infinite full-shell nanowire in the MHCM, for the parameters denoted by a dot in Fig. 1(d). It showcases a homogeneous nanowire, meaning that all its parameters are constant along the wire, particularly the chemical potential μ. We show half of the $n = 0$ and full $n = 1, 2$ LP lobes. We can observe a LP flux-modulated parent gap and below it, a number of bright features known as Caroli-de Gennes-Matricon (CdGM) analog states, described in Ref. 9. In the topological phase, as the one of Fig. 1(e), a bright signal appears at zero energy in the $n = 1$ LP, the MZM corresponding to the Majorana bound state schematically depicted in Fig. 1(c). Its flux-length is determined by the (μ, α) parameters given in Fig. 1(d). To isolate the MZM contribution, in Fig. 1(f) we show the $n = 1$ LDOS only for the $m_J = 0$ subband sector. Right at $\Phi_{\rm TT}$, we see the characteristic subband gap closing and reopening, signaling the TT and the appearance of the MZM. In the left corner of the $n = 1$ lobe the MZM disappears abruptly (without TT) due to the change of fluxoid. The phenomenology of MZMs in homogeneous nanowires has been extensively characterized in Ref. 10.

III. INHOMOGENEOUS WIRE

To model one of the frequent forms of disorder in hybrid nanowires, we will now add a smooth step-like chemical potential profile at the end of the full-shell nanowire (where typically a local probe is attached to measure, for instant, tunneling spectroscopy into the wire). It starts at a value μ_L at $z = 0$ and, within a distance $\sim \chi$, will smoothly transition to a value of μ_R for $z \geq 2L$ [see Fig. 2(e)]. This step-like profile defines two regions along the wire: one for $z \in [0, L)$, with $\mu \sim \mu_L$ (region L for left), and one for $z \in (L, \infty)$ with $\mu \sim \mu_R$ (region R for right). Each of these regions has, in a first approximation, its own TT flux, $\Phi_{\rm TT}^{L,R}$. Depending on which of the two is greater inside the first lobe, we will have qualitatively different behaviors.

A. Buried Majorana case

In Fig.2(a) we again show the topological phase diagram for the homogeneous wire of Fig. 1. With a white dashed curve, we highlight the values of (μ, α) for which L_Φ is maximum. We first consider the case where μ_L and μ_R are both *to the left* of this curve. Since by definition $\mu_L < \mu_R$, μ_R is in a brighter color spot than μ_L. Because of this, the TT of region L occurs at a smaller flux $\Phi_{\rm TT}^L$ than that of region R, $\Phi_{\rm TT}^R$.

In Fig. 2(b) we plot the total LDOS of the inhomogeneous nanowire calculated at $z = 0$. $\Phi_{\rm TT}^L < \Phi_{\rm TT}^R$ are

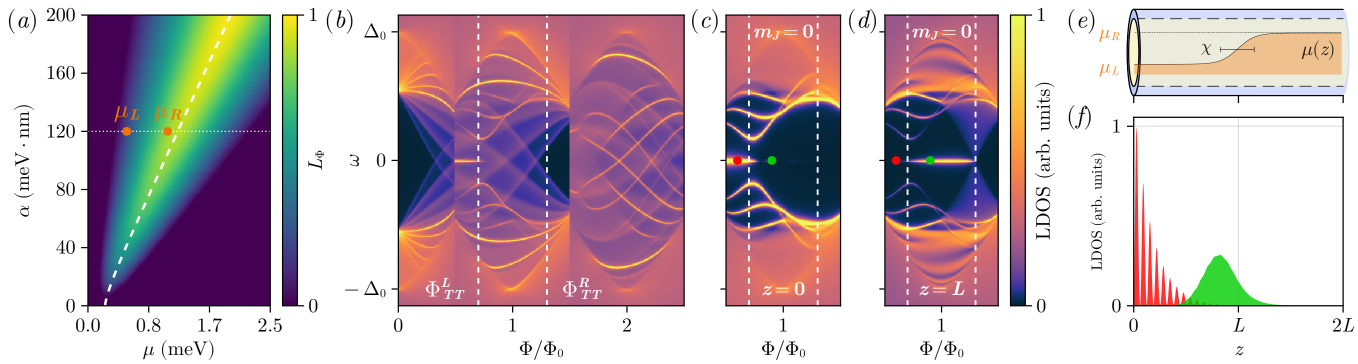

FIG. 2. **Inhomogeneous full-shell hybrid nanowire: Buried Majorana case.** (a) Topological phase diagram of a uniform full-shell hybrid nanowire, see Fig. 1(d). The white dashed line indicates the (μ, α) curve where the Majorana interval L_Φ is maximum. Red dots indicate two values of chemical potential, μ_L and μ_R (for the same α), taken *to the left* of the white dashed curve. (b) LDOS versus energy and normalized flux at the end ($z = 0$) of a semi-infinite nanowire with an inhomogeneous chemical potential profile along the z-direction. The $\mu(z)$ profile is schematically represented in panel (e). It consist of a smooth step between the μ_L and μ_R values indicated in (a) and is characterized by a smoothness parameter χ. It is located at a distance L close to the wire's end. In (b) we indicate with white dashed lines the bulk TT fluxes $\Phi^L_{\rm TT}$ and $\Phi^R_{\rm TT}$ associated with μ_L and μ_R, respectively (with $\Phi^L_{\rm TT} < \Phi^R_{\rm TT}$). (c) and (d) show the LDOS of the $n = 1$ LP lobe for the $m_J = 0$ subbands only, calculated at the wire's end $z = 0$ (c) and at the step center $z = L$ (d). (f) LDOS at $\omega = 0$ as a function of the coordinate z for two applied fluxes, indicated by colored dots in (c,d). Parameters: $L = 3000$ nm, $\chi = 250$ nm, $\mu_L = 0.53$ meV, $\mu_R = 1.09$ meV ($\Delta\mu = \mu_R - \mu_L = 0.56$ meV). Other parameters as in Fig. 1.

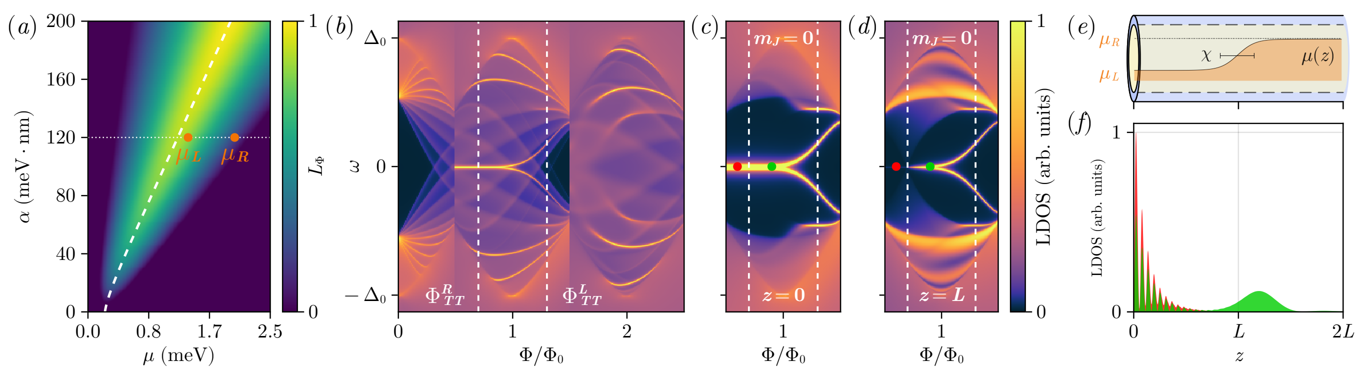

FIG. 3. **Inhomogeneous full-shell hybrid nanowire: Quasi-Majorana case.** Same as Fig. 2 but now μ_L and μ_R are taken *to the right* of the white dashed curve in (a), so that $\Phi^L_{\rm TT} > \Phi^R_{\rm TT}$. Parameters: $\mu_L = 1.37$ meV, $\mu_R = 2.01$ meV ($\Delta\mu = \mu_R - \mu_L = 0.64$ meV). Other parameters as in Fig. 2.

highlighted with vertical dashed lines. To distinguish more clearly the Majorana phenomenology from the one of the many CdGM analogs that coexist with the MZM, in Fig. 2(c) we show only the $m_J = 0$ contribution to the LDOS in the $n = 1$ LP lobe. We observe a MZM at the left end of the lobe. It disappears more or less at $\Phi^L_{\rm TT}$, where several subgap states give signals compatible with a gap closing and reopening. These states are nevertheless widely spaced out, corresponding to the finite length of region L. In Fig. 2(d) we plot an analogous $m_J = 0$ LDOS but at $z = L$. Now, the TT for region R is clearly visible at $\Phi^R_{\rm TT}$, in a similar fashion to the uniform semi-infinite wire case of Fig. 1(f). The MZM is however almost not visible to the left of $\Phi^L_{\rm TT}$.

Lastly, in Fig. 2(f) we plot a spatially-resolved LDOS for the $m_J = 0$, $\omega = 0$ states with flux values indicated by colored dots in (c,d). This LDOS provides a sense of the wave function profile of the zero-energy modes along the z coordinate. We see that for low flux values, both regions L and R are topological. The MZM is bound at the left end of the wire (red) just like in a semi-infinite homogeneous nanowire. As we increase the flux, however, region L departs from the topological condition, and eventually only region R becomes topological. In this process, the MZM moves from $z = 0$ toward the wire's interior and becomes bound to the chemical-potential defect around $z = L$ (green). Its shape depends on the smoothness parameter χ, but in general occurs for every χ. We call this the *buried* Majorana case and occurs approximately for half of parameter space in the topological region, whenever $\mu_{L,R}$ are to the left of the white dashed line in Fig. 2(a). A local probe at $z = 0$ is not capable of detecting the buried MZM, especially if $z = L$ is large, which is why in Fig. 2(c) no zero-energy state is observed at the green dot. It would only be detectable with a probe near $z = L$ [Fig. 2(d)].

B. Quasi-Majorana case

Now we take μ_L and μ_R *to the right* of the white dashed curve in Fig. 3(a). In Fig. 3 we perform a similar analysis to that in Fig. 2, but in this case we have $\Phi^L_{\rm TT} > \Phi^R_{\rm TT}$. In Fig. 3(c) we plot the $n = 1$ LDOS for the $m_J = 0$ sector at $z = 0$. We observe a zero-energy anomaly from the left of the lobe, all the way to approximately $\sim \Phi^L_{\rm TT}$. There, the zero-energy state disappears without signals of a TT. We just see that the bright feature goes away from zero until it merges with other higher-energy CdGM analogs close to the parent gap edge on the right of the $n = 1$ LP lobe. The equivalent LDOS at $z = L$ is shown in Fig. 3 (d). We observe two main differences with respect to (c). Now there is a conventional TT at $\Phi^R_{\rm TT}$, and no zero-energy mode can be detected for fluxes smaller than that value.

We can understand these features by plotting the spatially-resolved LDOS as before, see Fig. 3(f). At the red dot flux, the full wire is in the topological regime and a MZM is bound to the left end, as in the homogeneous full-shell nanowire. This Majorana is detected in Fig. 3(c), but is almost invisible when the local probe is at $z = L$, Fig. 3(d). In contrast, at the green dot flux, we have a zero-energy state with spectral weight at both $z = 0$ and $z = L$. It is composed of two features along the wire: one at the wire's end, resembling the MZM red wave function that corresponds to an abruptly terminated nanowire, and another at around the chemical potential step, with a smooth spatial profile. This is called the *quasi-Majorana* case and was analyzed in detail in conventional Zeeman-driven Majorana nanowires [5]. In this case, the whole nanowire is in the trivial state. Reducing the flux from the right of the $n = 1$ lobe, we can see a subgap state that decreases its energy until it is pinned to zero energy close to $\Phi^L_{\rm TT}$. This is a characteristic feature of a quasi-Majorana as its energy approaches zero as [14]

$$\omega_{\rm QMJ} \sim \Delta_0 e^{-\frac{V_Z^{\phi\,3}}{\hbar\alpha\Delta_0}\frac{\chi}{\Delta\mu}}. \tag{9}$$

It gets closer to zero energy for a smaller step of the chemical potential $\Delta\mu = \mu_R - \mu_L$ and for smoother spatial variation χ.

IV. CONCLUSIONS

We have analyzed the fate of MZMs in inhomogeneous full-shell hybrid nanowires, particularly when there is a smooth chemical potential step $\Delta\mu = \mu_R - \mu_L$ close to the wire's end. We have found two typical scenarios depending on whether μ_L and μ_R are *to the left* or *to the right* of the topological phase-diagram center (expressed as a function of SOC α and chemical potential μ). In the first scenario, the buried Majorana case, a MZM bound to the wire's end at small fluxes (within the first LP lobe), shifts toward the wire's interior as the flux increases and cannot be detected anymore through local spectroscopy at $z = 0$. In this case, a part of the nanowire is always in the topological regime. In the second scenario, a zero-energy anomaly is always detected at $z = 0$, but it can be topological or trivial, without any revealing signature in LDOS. This is the quasi-Majorana case. It is dangerous because the whole wire can be in the trivial regime, but the presence of smoothly confined quasi-Majorana modes can mimic the local features of true MZMs. According to our numerical simulations, there is approximately a 50% chance of being in one scenario or another.

[1] A. Y. Kitaev, Unpaired Majorana fermions in quantum wires, Physics-Uspekhi **44**, 131 (2001).
[2] S. D. Sarma, M. Freedman, and C. Nayak, Majorana zero modes and topological quantum computation, npj Quantum Inf **1**, 1 (2015).
[3] Y. Oreg, G. Refael, and F. Von Oppen, Helical Liquids and Majorana Bound States in Quantum Wires, Physical Review Letters **105**, 177002 (2010).
[4] R. M. Lutchyn, J. D. Sau, and S. Das Sarma, Majorana Fermions and a Topological Phase Transition in Semiconductor-Superconductor Heterostructures, Physical Review Letters **105**, 077001 (2010).
[5] E. Prada, P. San-Jose, M. W. A. d. Moor, A. Geresdi, E. J. H. Lee, J. Klinovaja, D. Loss, J. Nygård, R. Aguado, and L. P. Kouwenhoven, From Andreev to Majorana bound states in hybrid superconductor-semiconductor nanowires, Nature Reviews Physics **2**, 575 (2020).
[6] S. Vaitiekėnas, G. W. Winkler, B. van Heck, T. Karzig, M.-T. Deng, K. Flensberg, L. I. Glazman, C. Nayak, P. Krogstrup, R. M. Lutchyn, and C. M. Marcus, Flux-induced topological superconductivity in full-shell nanowires, Science **367**, eaav3392 (2020).
[7] W. A. Little and R. D. Parks, Observation of Quantum Periodicity in the Transition Temperature of a Superconducting Cylinder, Physical Review Letters **9**, 9 (1962).
[8] R. D. Parks and W. A. Little, Fluxoid Quantization in a Multiply-Connected Superconductor, Physical Review **133**, A97 (1964).
[9] P. San-Jose, C. Payá, C. M. Marcus, S. Vaitiekėnas, and E. Prada, Theory of caroli–de gennes–matricon analogs in full-shell hybrid nanowires, Phys. Rev. B **107**, 155423 (2023).
[10] C. Payá, S. D. Escribano, A. Vezzosi, F. Peñaranda, R. Aguado, P. San-Jose, and E. Prada, Phenomenology of Majorana zero modes in full-shell hybrid nanowires, Physical Review B **109**, 115428 (2024).
[11] P. San-Jose, pablosanjose/Quantica.jl: v1.1.0 (2024).
[12] C. Payá, CarlosP24/FullShell.jl: Full-shell semi-infinite nanowire Hamiltonian builder - destructive LP improved (2024).
[13] S. Danisch and J. Krumbiegel, Makie.jl: Flexible high-performance data visualization for Julia, Journal of Open Source Software **6**, 3349 (2021).
[14] G. Kells, D. Meidan, and P. W. Brouwer, Near-zero-energy end states in topologically trivial spin-orbit coupled superconducting nanowires with a smooth confinement, Physical Review B **86**, 100503 (2012).